

Lie Access Neural Turing Machine

Greg Yang^a *

^a*Harvard University*

May 29, 2022

Abstract

Recently, Neural Turing Machine and Memory Networks have shown that adding an external memory can greatly ameliorate a traditional recurrent neural network’s tendency to forget after a long period of time. Here we present a new design of an external memory, wherein memories are stored in an Euclidean *key space* \mathbb{R}^n . An LSTM controller performs read and write via specialized structures called read and write heads, following the design of Neural Turing Machine. It can move a head by either providing a new address in the key space (aka random access) or moving from its previous position via a Lie group action (aka Lie access). In this way, the “L” and “R” instructions of a traditional Turing Machine is generalized to arbitrary elements of a fixed Lie group action. For this reason, we name this new model the Lie Access Neural Turing Machine, or LANTM.

We tested two different configurations of LANTM against an LSTM baseline in several basic experiments. As LANTM is differentiable end-to-end, training was done with RMSProp. We found the right configuration of LANTM to be capable of learning different permutation and arithmetic tasks and extrapolating to at least twice the input size, all with the number of parameters 2 orders of magnitude below that for the LSTM baseline. In particular, we trained LANTM on addition of k -digit numbers for $2 \leq k \leq 16$, but it was able to generalize almost perfectly to $17 \leq k \leq 32$.

1 Introduction

Recurrent neural networks (RNNs) are powerful devices that, unlike conventional neural networks, are able to keep state across time. They have obtained profound achievements in diverse arenas like machine translation [15, 3, 1], speech recognition [4, 2], image captioning [13, 10, 16], and so on. However, despite such advances, RNNs still cannot maintain memory for long periods of time, presenting an obstacle to attaining human-like general intelligence.

Recently, the Neural Turing Machine (NTM) of Graves et al. [5] and memory networks of Sukhbaatar et al. [14] achieved breakthroughs toward this goal by utilizing external memories. This capability allowed NTM to learn and generalize simple algorithms, and the memory network to complete simple QA tasks. Later on, Grefenstette et al. [6] introduced neural stacks, queues, and dequeues. It followed in the trend for external memories: as NTM’s external memory could be treated as a smooth version of a random access memory array, neural stack/queues/deques could be treated as smooth versions of the corresponding discrete data structures, to be operated by LSTM controllers. These models were able to learn language-like tasks over very long input sequences and generalize to even longer sequences.

We here present a new design of an external memory based on a dictionary with keys residing in an Euclidean *key space* \mathbb{R}^n . Read and write heads move around in this key space either by random

*email: gyang@college.harvard.edu

access or via an action of a fixed Lie group G and perform their functions with the current address. In analogy to the traditional Turing machine, the tape has become a continuous space and the “L” and “R” movement instructions have become elements of G .

Combining this external memory with an LSTM controller, we call such a model Lie Access Neural Turing Machine, or LANTM.

With a concrete implementation with the key space being \mathbb{R}^2 and G being the translation group, we show that LANTM, with the right design choices, learns simple algorithms and generalizes very well. In particular, it learns addition of ≤ 16 digit integers but can answer 99% of randomly selected ≤ 32 digit addition problems correctly. Furthermore, while the same model trained on ≤ 16 digit addition could no longer correctly compute 64 digit additions, the outputs given are only wrong in a small fraction (5%) of total digits.

2 Background

2.1 Lie groups

We here review basic concepts of (Lie) group theory.

A **group** is a set S with operations $*$ (multiplication), $(.)^{-1}$ (inverse), and e (unit) of arity respectively 2, 1, 0, such that

- (associativity) for all $a, b, c \in G$, $(a * b) * c = a * (b * c)$
- (inverse) for all $a \in G$, $a * a^{-1} = a^{-1} * a = e$
- (identity) for all $a \in G$, $a * e = e * a = a$

The classical examples are $(\mathbb{Z}^n, +, -(\cdot), 0)$, $(\mathbb{R}^n, +, -(\cdot), 0)$, matrix groups like $\text{GL}(n)$, and cyclic groups $\mathbb{Z}/n\mathbb{Z}$.

A group often “acts on” another object or set, like a hand twists a rubik’s cube. For example, imagine an equilateral triangle with its vertices colored differently. Rotating the triangle by 120 degrees permutes the vertex color but leaves the overall shape unchanged. If we let $0, 1, 2 \in \mathbb{Z}/3\mathbb{Z}$ correspond respectively to rotations of the equilateral triangle by 0, 120, or 240 degrees, and addition in $\mathbb{Z}/3\mathbb{Z}$ corresponds to applying two such rotations consecutively, then $\mathbb{Z}/3\mathbb{Z}$ is said to act on the set of color permutations of the triangle, because it maps one such permutation to another by a rotation. Or, consider $A = \mathbb{R}^2$ as a set of vectors and $B = \mathbb{R}^2$ as a set of points. One may drag an element of B by a vector from A , thus mapping it to another element of B . Then we say A acts on B by vector addition. As this example illustrates, a group G always acts on itself by the group multiplication (in the example, this is addition of \mathbb{R}^2 vectors). So in fact, every group acts on another set. Formally, a *group action* of group G on set X is defined as a mapping $\phi : G \times X \rightarrow X : (g, x) \mapsto g \cdot x$ such that

- $e \cdot x = x$ for all $x \in X$
- $(a * b) \cdot x = a \cdot (b \cdot x)$ for all $a, b \in G, x \in X$.

It is the ubiquity of group action that explains the ubiquity of groups in mathematics. In this paper, we only borrow the language of groups and group actions to the extent it neatly expresses many ideas central to our design. No advanced ideas from mathematics are used.

A *Lie group* is a group with a smooth manifold structure such that multiplication and inverse operations are smooth maps. Similarly, a *smooth group action* of a Lie group G on smooth manifold M is just a group action $\phi : G \times M \rightarrow M$ that is smooth. In the context of smooth Lie group action, we also call elements of G *Lie actions*.

The reader who has had no experience with smooth topology need not worry too much about the precise meaning of these definitions beyond the intuition that “Lie group is a group such that

most things you do to it are differentiable” and “smooth Lie group action is a differentiable group action”. Indeed, the only reason we require a Lie group rather than a group is so that its group action yields to gradient descent. (To that end, it is not strictly necessary for the groups to be infinitely differentiable, but as all common differentiable groups are Lie groups and all groups explored in this paper are Lie group, this distinction is not needed.) The reader hoping to learn the basics of smooth manifolds and Lie groups can consult John Lee’s excellent *Introduction to Smooth Manifolds* [12].

2.2 Recurrent Neural Networks

Unlike the conventional feedforward neural network, a recurrent neural network (RNN) has self-connections. In other words, it maintains an internal state similar to the latent variables of a hidden Markov model.

Mathematically, an RNN is a function $\rho : X \times H \rightarrow Y \times H$, where X is the input space, Y the output space, and H the space of internal states. On input $(x^{(1)}, \dots, x^{(T)}) \in X^T$ and with initial state $h^{(0)} \in H$, the RNN transitions into states $h^{(1)}, \dots, h^{(T)}$ (internally) and returns a sequence $(y^{(1)}, \dots, y^{(T)})$ (externally) defined recursively by

$$(y^{(t)}, h^{(t)}) = R(x^{(t)}, h^{(t-1)}).$$

A simple implementation of R would just be a 2-layer neural network

$$\begin{aligned} h^{(t)} &:= \tau(W_{xh}x^{(t)} + W_{hh}h^{(t-1)} + b_h) \\ y^{(t)} &:= W_{hy}h^{(t)} + b_y \end{aligned}$$

where τ is a transfer function, $W_{..}$ are matrices and $b_{..}$ are bias vectors.

τ is usually differentiable everywhere or almost everywhere, so that the RNN can be trained by backpropagation through time (BPTT) [17].

In this work, we use a particular variant of RNN called the Long Short Term Memory (LSTM) [7]. LSTM’s hidden state consists of two variables $(c^{(t)}, h^{(t)})$, where $h^{(t)}$ is also the output to the external world (i.e. it fills the role of $y^{(t)}$ in the above description). The $c^{(t)}$ is the “memory” of the machine, designed to be maintained for a long time when necessary. There are many variants of LSTM. In this paper we define the function $\text{LSTM} : (x^{(t)}, c^{(t-1)}, h^{(t-1)}) \mapsto (y^{(t)}, c^{(t)}, h^{(t)})$ as follows:

$$\begin{aligned} i^{(t)} &:= \sigma(W_{xi}x^{(t)} + W_{hi}h^{(t-1)} + b_i) \\ f^{(t)} &:= \sigma(W_{xf}x^{(t)} + W_{hf}h^{(t-1)} + b_f) \\ c^{(t)} &:= f^{(t)}c^{(t-1)} + i^{(t)} \tanh(W_{xc}x^{(t)} + W_{hc}h^{(t-1)} + b_c) \\ o^{(t)} &:= \sigma(W_{xo}x^{(t)} + W_{ho}h^{(t-1)} + b_o) \\ h^{(t)} &:= o^{(t)} \tanh(c^{(t)}) \\ y^{(t)} &:= h^{(t)} \end{aligned}$$

where σ is the logistic function. $i^{(t)}, f^{(t)}, o^{(t)}$ are called the input, forget, and output gates, respectively, which modulate multiplicatively different quantities in the computation. The weights $W_{..}$ are trainable through BPTT. The undashed parts of figure 1 show a schematic of the equations above.

In models with external memories, LSTM often serves as the controller [5, 6, 20]. This means that 1) the entire system carries state over time from both the LSTM and the external memory, 2) the LSTM controller collects reading from and computes additional instructions to the external memory, and 3) the LSTM possibly performs extra processing F to return the desired output at each time point. The dashed parts of figure 1 demonstrate a typical such arrangement, in which $\Sigma^{(t)}$ represents the state of the memory, $\rho^{(t)}$ represents the reading from the memory, RW represents a

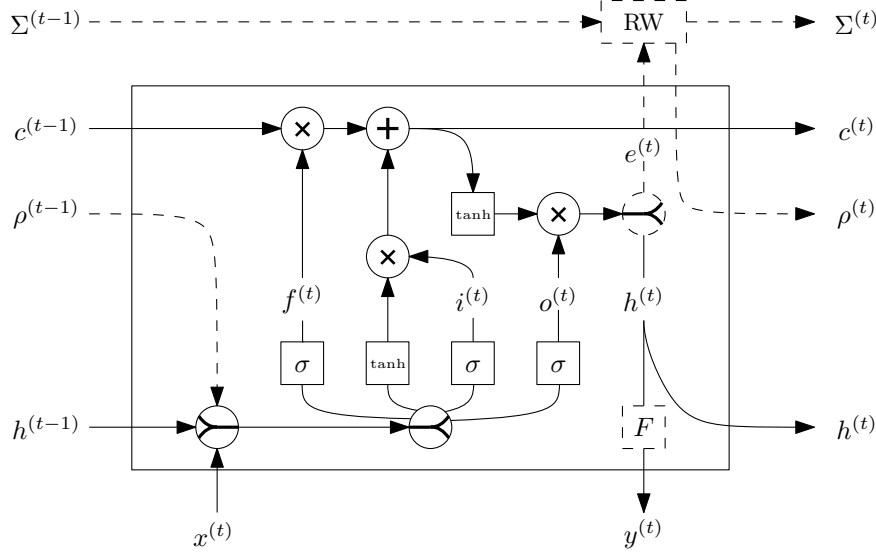


Figure 1: LSTM schematics, with and without external memory. A plain LSTM is illustrated by the undashed part of the diagram. LSTM as a controller of an external memory is illustrated by including the dashed parts. The \succ gate indicates concatenating inputs and applying a linear transformation given by the weights of the network. The \prec gate indicates the splitting of a vector. F is any processing of $h^{(t)}$ to produce the final output $y^{(t)}$, e.g. a softmax to produce a distribution over vocabulary.

subroutine used for reading from and writing to the memory. The entire system is now described by the recurrence $\text{TM} : (x^{(t)}, \Sigma^{(t-1)}, c^{(t-1)}, \rho^{(t-1)}, h^{(t-1)}) \mapsto (y^{(t)}, \Sigma^{(t)}, c^{(t)}, \rho^{(t)}, h^{(t)})$ defined by

$$\begin{aligned} (e^{(t)} \oplus h^{(t)}, c^{(t)}, e^{(t)} \oplus h^{(t)}) &:= \text{LSTM}(x^{(t)}, c^{(t-1)}, \rho^{(t-1)} \oplus h^{(t-1)}) \\ y^{(t)} &:= F(h^{(t)}) \\ (\Sigma^{(t)}, \rho^{(t)}) &:= \text{RW}(\Sigma^{(t-1)}, e^{(t)}), \end{aligned}$$

where $e^{(t)}$ is a set of instructions to read from and write to the memory, as illustrated in figure 1. F is usually a softmax layer that produces a distribution over all possible symbols in a language task such as those explored in this paper, and this is indeed the case with LANTM. In the next section, we show how LANTM implements RW.

3 Lie Access Memory

As mentioned in the introduction, Lie Access Neural Turing Machine (LANTM) is based off of the external memory architecture of Neural Turing Machine (NTM). This architecture can be summarized by figure 2: a neural network controller reads from and writes to a memory structure via specially designed functions called “heads”, paying respect to terminologies of Turing machine literature. The heads themselves do not have any trainable parameters, so the only learning done is by the controller.

In a LANTM, the memory structure is a dictionary, with keys in an Euclidean space \mathbb{R}^n for a fixed n , called the *key space* or *address space*; and with values (called *memory vectors*) in another Euclidean space \mathbb{R}^m for a fixed m (m is called the *memory width*). At time step t , each read head converts instructions from the controller to a read address $k_r^{(t)} \in \mathbb{R}^n$ that retrieves a reading $\rho^{(t)}$ from the memory by a weighted inverse squared (or polynomial in general) law, to be elaborated below. Each write head converts instructions from the controller to a new memory vector $m^{(t)} \in \mathbb{R}^m$

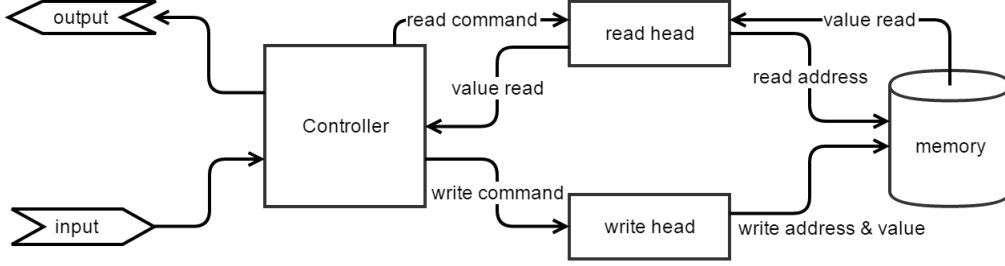


Figure 2: Abstract diagram of an external memory architecture. Note that unlike the other diagrams in this paper (which are unfolded in time), the connections displayed here are recurrent.

and a new address $k_w^{(t)} \in \mathbb{R}^n$, along with a scalar $s^{(t)} \in [0, 1]$, called the *memory strength* of the vector. Such a triple $(k_w^{(t)}, m^{(t)}, s^{(t)})$ is essentially appended to the memory.

Aside from m and n , another hyperparameter of a LANTM is its choice of Lie group G that acts on \mathbb{R}^n . At time $t + 1$, the controller may emit new addresses for each head (random access) or issue Lie actions $g \in G$ that change the old addresses (Lie access).

One may imagine the key space to be a piece of paper, and the read and write heads to be stones placed on this paper. The controller is a hand that moves the stones from turn to turn. Sometimes it may lift a stone up and place it somewhere completely unrelated to its original position (random access); other times it may drag a stone along a chosen direction (Lie access).

In the design discussed in this paper, there is no explicit erasure. However, the machine can theoretically store the exact negation of a memory vector at the same location to cancel out that memory, albeit the required precision to do so would probably be overwhelming.

What follows are details of the overview given above.

3.1 Read

Let $M^{(t)}$ denote the set of memory vectors stored in the key space by time t . We choose a canonical ordering on this set, for example by time added, and write $M^{(t)}(i)$ for the i th vector in this order. Denote by $a^{(t)}(i)$ the corresponding addresses of $M^{(t)}(i)$ and by $S^{(t)}(i)$ the corresponding memory strength of $M^{(t)}(i)$. In this section we introduce two *weight schemes* for retrieving a value from the memory via an address. The main idea of both is summarized by figure 3.

The read key $k_r^{(t)}$ produces weightings $w_r^{(t)}(i)$ over all memory vectors $M^{(t)}(i)$, each with address $a^{(t)}(i)$, by normalizing their inverse squared distances:

$$w_r^{(t)}(i) := \frac{S^{(t)}(i) \|k_r^{(t)} - a^{(t)}(i)\|^{-2}}{\sum_j S^{(t)}(j) \|k_r^{(t)} - a^{(t)}(j)\|^{-2}}$$

with the convention that it takes the limit value when $k_r^{(t)} \rightarrow a^{(t)}(i)$ for some i (e.g. if all the keys are distinct and all strengths are nonzero, then $w_r^{(t)}(i) = 1$ and $w_r^{(t)}(j) = 0$ for $j \neq i$).

In practice, as the formula for $w_r^{(t)}$ can induce numerical instability as $k_r^{(t)} \rightarrow a^{(t)}(i)$ for some i , we adjust the formula with a small ϵ , e.g. 10^{-9} , so that

$$w_r^{(t)}(i) := \frac{S^{(t)}(i) (\|k_r^{(t)} - a^{(t)}(i)\|^2 + \epsilon)^{-2}}{\sum_j S^{(t)}(j) (\|k_r^{(t)} - a^{(t)}(j)\|^2 + \epsilon)^{-2}}.$$

Obviously, $\sum_j w_r^{(t)}(j) = 1$ and each $w_r^{(t)}(i)$ is nonnegative, so the reading

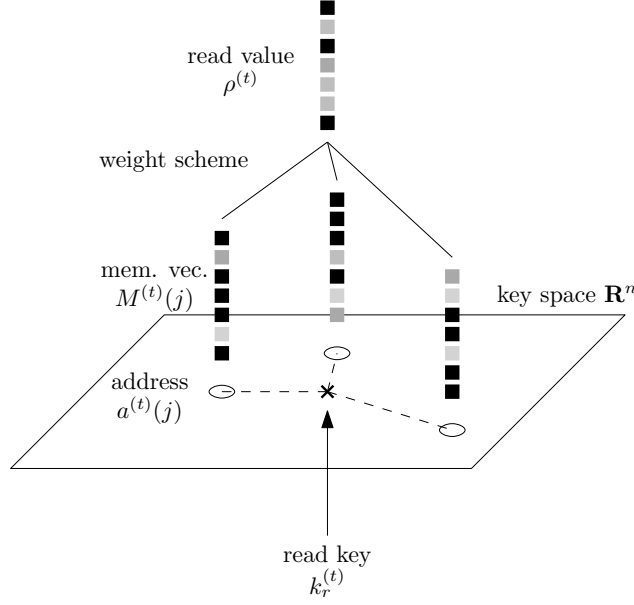


Figure 3: Retrieval of value from memory via a key. Weightings with unit sum are assigned to different memories depending on the distances from the addresses to the read key. The weighted arithmetic mean is emitted as the final read value. Both InvNorm and SoftMax schemes follow this method, but each with a different way of computing the weightings. In particular, the SoftMax scheme requires another input, the temperature $T^{(t)}$.

$$\rho^{(t)} := \sum_j w_r^{(t)}(j) M^{(t)}(j)$$

is a convex combination of the stored memories.

In general, the 2 in the power of the absolute distances can be replaced by any exponent $\alpha > 0$ to yield

$$w_{r\alpha}^{(t)}(i) := \frac{S^{(t)}(i) \|k_r^{(t)} - a^{(t)}(i)\|^{-\alpha}}{\sum_j S^{(t)}(j) \|k_r^{(t)} - a^{(t)}(j)\|^{-\alpha}}.$$

We call this method of converting a read key to a set of weighting via a polynomial law *InvNormalize*, or *InvNorm* for short, in contrast with the use of exponential law in the case of SoftMax weight scheme, which computes the weights $w_r^{(t)}(i)$ as

$$w_r^{(t)}(i) := \frac{S^{(t)}(i) \exp(-\|k_r^{(t)} - a^{(t)}(i)\|^2/T^{(t)})}{\sum_j S^{(t)}(j) \exp(-\|k_r^{(t)} - a^{(t)}(j)\|^2/T^{(t)})}$$

where $T^{(t)}$ is a *temperature* emitted by the controller at time t that represent the certainty of its reading. The higher $T^{(t)}$ is, the more $w_r^{(t)}$ tends to the uniform distribution.

Given the ubiquity of SoftMax in the machine learning literature, one may consider it a natural choice for the weight scheme. But as will be seen in the experiments, InvNorm is crucial in making the Euclidean space work as an address space.

3.2 Write

There is no extra ingredient to writing other than adding the produced memory vector $m^{(t)}$, its strength $s^{(t)}$, and its address $k_w^{(t)}$ to the collection of memory vectors, strengths, and addresses.

To ensure that memory selection by weighted average works well, we squash the values of $m^{(t)}$ to $[-1, 1]$ by \tanh , but squashing by the logistic sigmoid function is also conceivable. Without such squashing, a memory vector $M^{(t)}(i)$ with large values can dominate the output of a weight method despite having low weight $w_r^{(t)}(i)$.

3.3 Addressing procedure

Here we describe how the keys $k_r^{(t)}$ and $k_w^{(t)}$ are produced. The procedure is the same for both read and write keys, so we assume that we are to compute a single key $k^{(t)}$.

We first describe the abstraction of the process over any fixed Lie group G acting smoothly on the key space \mathbb{R}^n . In particular, the exact mechanism for producing an element of G is left unspecified at the moment. In the next few subsections we discuss the particular choices of G .

The controller emits 3 things: a *candidate key* $\tilde{k}^{(t)} \in \mathbb{R}^n$, a *mixing coefficient*, or *gate*, $g^{(t)} \in [0, 1]$, and an action $v^{(t)} \in G$ that we also call *step*.

The gate g mixes the previous key $k^{(t-1)}$ with the candidate key to produce a *pre-action key* $\bar{k}^{(t)}$, which is transformed by $v^{(t)}$ to produce the final key $k^{(t)}$

$$\begin{aligned}\bar{k}^{(t)} &:= g^{(t)}\tilde{k}^{(t)} + (1 - g^{(t)})k^{(t-1)} \\ k^{(t)} &:= v^{(t)} \cdot \bar{k}^{(t)}\end{aligned}$$

where \cdot denotes group action.

3.3.1 Example: The scaling rotation group $\mathbb{R}^* \times \text{SO}(2)$

The scaling rotation group $\mathbb{R}^* \times \text{SO}(2)$ is the group of linear transformations of \mathbb{R}^2 that decomposes into a rotation followed by a dilation (or contraction).

In the specific case of $G = \mathbb{R}^* \times \text{SO}(2)$, the controller would produce 2 numbers $a = a^{(t)}$, $b = b^{(t)}$, which represents the element

$$v = \begin{pmatrix} a & -b \\ b & a \end{pmatrix}$$

of the group. The matrix acts on a key $k = (x, y)^T \in \mathbb{R}^2$ by left matrix multiplication

$$v \cdot k = \begin{pmatrix} a & -b \\ b & a \end{pmatrix} \begin{pmatrix} x \\ y \end{pmatrix}$$

This is the same as scaling by the scalar $c = \sqrt{\|a\|^2 + \|b\|^2}$ and then rotating (i.e. left multiplication) by the orthogonal matrix

$$\begin{pmatrix} a/c & -b/c \\ b/c & a/c \end{pmatrix}$$

Another viewpoint is to treat $(a, b) \in \mathbb{R}^2 - \{0\}$ as the complex number $a + bi \in \mathbb{C} - \{0\}$. Then one can view the action $v \cdot k$ for $k = (x, y)^T \in \mathbb{R}^2$ as the complex multiplication $(a + bi)(x + yi)$.

3.3.2 Example: The rotation group $\text{SO}(2)$

The rotation, or special orthogonal, group $\text{SO}(2)$ is as its name suggests, the group of all linear transformations of \mathbb{R}^2 expressible as a rotation.

When $G = \text{SO}(2)$, we can just modify the scheme from the last example by scaling (a, b) to unit norm, $(\bar{a}, \bar{b}) = (a, b)/c$. The rest will follow just the same.

3.3.3 Example: The translation group \mathbb{R}^2 acting on \mathbb{R}^2

The case of the translation group is simpler. Again the controller outputs 2 numbers $a = a^{(t)}, b = b^{(t)}$, so that $v = (a, b)$ acts upon a key $k = (x, y)$ by

$$v \cdot k = (x, y) + (a, b) = (x + a, y + b)$$

3.4 Interpolation of Lie action

For groups like $(\mathbb{R}^n, +)$, there is a well-defined convex interpolation between two elements that stays in the group. For some others like $\mathbb{R}^* \times \text{SO}(2)$, the straight-line interpolation $tv + (1-t)w$ for $t \in [0, 1]$, $v, w \in G$ sometimes produce elements outside the group (in this case sometimes the elements cancel out and get 0), but does so with probability zero in a suitable sense.

Then, as for keys, we can let the controller output a candidate action $\tilde{v}^{(t)} \in G$ and a mixing coefficient $h^{(t)}$ to smoothly mix with the previous action $v^{(t-1)}$ to produce a final action

$$v^{(t)} := h^{(t)}\tilde{v}^{(t)} + (1 - h^{(t)})v^{(t-1)}.$$

This allows the controller to “move in a straight line within the group of actions” by merely left saturating (i.e. squash to 0) the gates $g^{(t)}$ and $h^{(t)}$ for all t , so that $v^{(1)} = v^{(2)} = v^{(3)} = \dots$. Of course, the “straight line” can be actually curved depending on the group. For example, when $G = \mathbb{R}^* \times \text{SO}(2)$, a typical “straight line” will be a spiral tending exponentially toward the origin or growing exponentially unbounded. In a more precise mathematical terminology, the keys of the read/write head will be on the orbit of the initial key by a \mathbb{Z} -parametrized subgroup of G .

Even if a group doesn’t have a natural straight-line interpolation, there may be another way to mix two actions. In the case of $G = \text{SO}(2) \cong S^1$, we can just project a straight-line interpolation onto the circle (barring a measure zero chance of interpolating into $(0, 0) \in \mathbb{R}^2$).

The method of geodesics allow for interpolation between a wider class of Lie groups, like compact groups, but it may be too unwieldy and slow. In the end, any interpolation method should be dictated by performance first.

The final addressing mechanism is shown in figure 4.

All together, the interaction of the controller with the external memory is shown in figure 5.

4 Experiments

The baselines of our experiments are LSTMs in an encoder-decoder setup as described in [15]. We tested 2 variations of LANTM with an InvNorm and a SoftMax address mechanism, along with the LSTM baseline, on the permutation and arithmetic tasks to be described. The Lie group for both types of LANTM is the translation group \mathbb{R}^2 acting on \mathbb{R}^2 ¹. For both LANTMs and LSTM, we embed the input vocabulary continuously via a real embedding matrix into an Euclidean space before feeding into the models; we also pass the outputs through a softmax layer to arrive at probability distributions over the vocabulary set (this is the F box in figure 1). As usual, prediction is performed via argmax but training is done by minimizing negative log likelihood.

The machines are first fed a learnable initial state and then provided with the input sequence, flanked by a start-of-input (SOI) symbol $\langle s \rangle$ and a repetition of an end-of-input (EOI) symbol $\langle /s \rangle$. The machines are to output the correct sequence during the *response phase*, which starts when they receive the first $\langle /s \rangle$. The repetition of $\langle /s \rangle$ effectively ensures that the correct symbols are not shown to the machines during answering. The machine also must correctly emit an end-of-output

¹We early on experimented with the scaling rotation group $\mathbb{R}^* \times \text{SO}(2)$, which produced acceptable results when input lengths were small but encountered numerical problems when input lengths were large due to exponentiating scale.

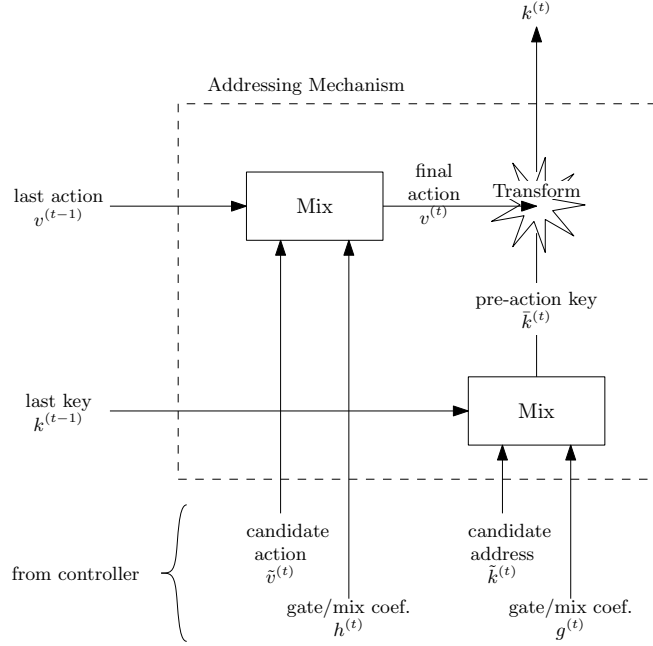


Figure 4: addressing mechanism.

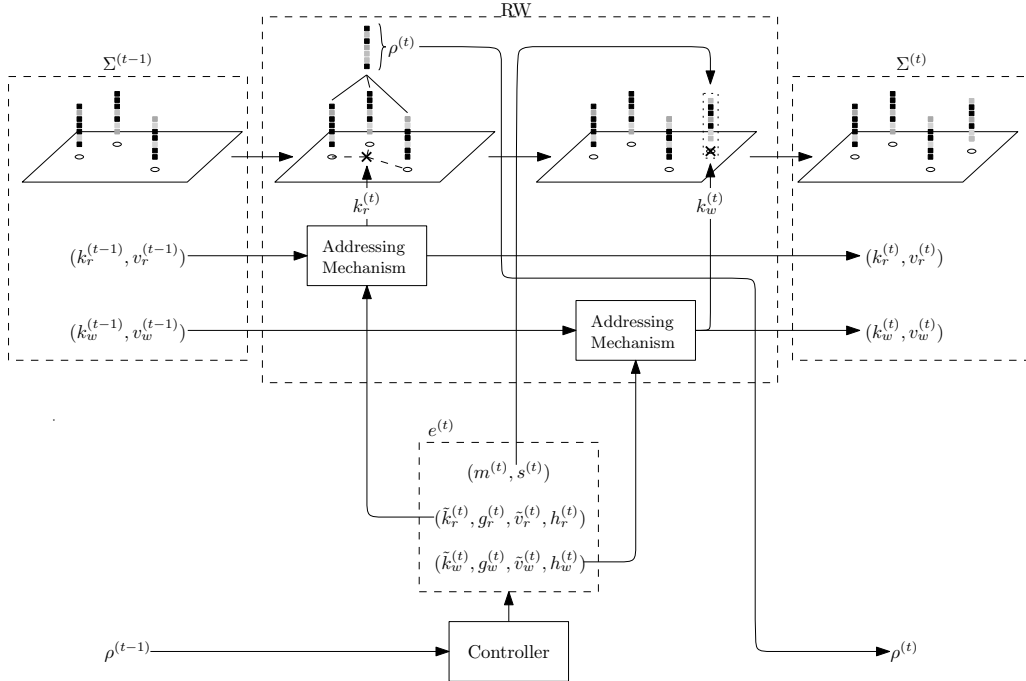


Figure 5: Summary of controller interaction with external memories. The dashed boxes correspond to dashed parts in figure 1. Note that all input, output and the states of the LSTM other than $\rho^{(t)}$ have been omitted.

(EOO) symbol $\langle e \rangle$ to terminate their answers. Figure (6) is an example of inputs and correct outputs during a copy task.

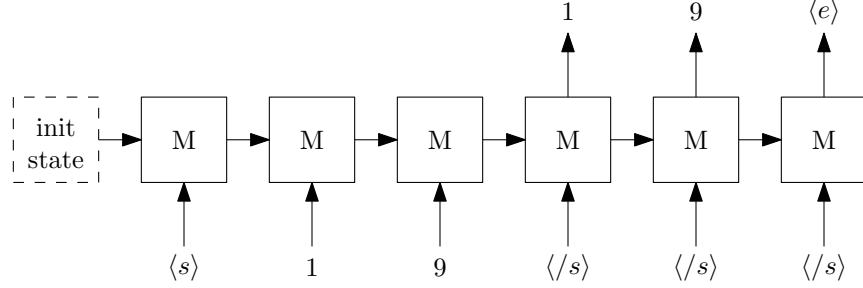


Figure 6: example in/out schematic.

Tasks. Each task has a length parameter k . The permutation tasks include

1. copy

input: $a_1 a_2 a_3 \cdots a_k$
output: $a_1 a_2 a_3 \cdots a_k$

2. reverse

input: $a_1 a_2 a_3 \cdots a_k$
output: $a_k a_{k-1} a_{k-2} \cdots a_1$

3. bigramFlip

input: $a_1 a_2 a_3 a_4 \cdots a_{2k-1} a_{2k}$
output: $a_2 a_1 a_4 a_3 \cdots a_{2k} a_{2k-1}$

The arithmetic tasks include the following. Note that all numbers, input or output, are formatted with the least significant digits **on the left** and with zero padding.

1. double. Let x be an integer in the range $[0, 10^k]$, with zero padding in front (on the right) to make up k digits.

input: x in base 10, zero padded to k digits
output: $2x$ in base 10, zero padded to $k + 1$ digits

2. addition. Let x and y be integers in the range $[0, 10^k]$, with zero padding in front (on the right) to make up k digits. If they have digits $x_1 x_2 \cdots x_k$ and $y_1 y_2 \cdots y_k$, respectively, with the *least* significant digits on the left, then

input: $x_1 y_1 x_2 y_2 \cdots x_k y_k$
output: $x + y$ in base 10, zero padded to $k + 1$ digits, with least significant digits on the left

In other words, we interleave the inputs. Thus this is a different encoding of the addition problem from previous works like [19] and [8].

task	min train	max train	min test	max test
copy	2	64	65	128
reverse	2	64	65	128
bigramFlip	2	32	33	64
double	2	40	41	80
addition	2	16	17	32

Table 1: Input sizes for each task. For permutation tasks, the numbers indicate input sequence length. For arithmetic tasks, the numbers indicate number of digits of (each) input. Thus for the addition task, “16” means that an input of 2 16-digit numbers.

Model	Task	LSTM size	Vocab	Embed.	Mem. width	LR	#Param
LANTM InvNorm	copy	50	128	7	20	0.02	26105
	reverse	50	128	7	20	0.02	26105
	bigramFlip	100	128	7	20	0.02	70155
	addition	50	14	14	20	0.01	20291
	double	50	14	7	20	0.02	18695
LANTM SoftMax	copy	50	128	7	20	0.02	26156
	reverse	50	128	7	20	0.02	26156
	bigramFlip	100	128	10	20	0.02	72123
	addition	50	14	14	20	0.01	20291
	double	50	14	14	20	0.02	20291
LSTM	copy	4×256	128	7	NA	0.0002	1918222
	reverse	4×256	128	7	NA	0.0002	1918222
	bigramFlip	4×256	128	7	NA	0.0002	1918222
	addition	4×256	14	64	NA	0.0002	1918222
	double	4×256	14	64	NA	0.0002	1918222

Table 2: Parameters in each model. “Vocab” is the size of the vocabulary (i.e. the total number of possible characters of each input sequence). “Embed” is the dimension of the embedding space. For example, if “Embed” is 7, then each character is mapped to a vector in \mathbb{R}^7 . “Mem. width” is the size of each memory vector. “LR” is the learning rate. “#Param” gives the total number of trainable parameters.

Task parameters and hyperparameters. We trained the models on the above tasks for input sizes summarized by table 1. For all tasks, the LANTM has a single-layer, 50-cell or 100-cell LSTM controller. The Lie group for all LANTMs is the translation group \mathbb{R}^2 acting on the key space \mathbb{R}^2 , as mentioned above. The memory width (i.e. the size of each memory vector) is 20. For all tasks, the LSTM baseline has 4 layers, each with 256 cells. The exact setting of parameters for each model in each task is listed in table 2.

Training and testing. We seek to minimize the negative log likelihood of the individual output characters given the input

$$\text{NLL}(\mathbf{W}) := \sum_{i=1}^L -\log \Pr[y_i = \tilde{y}_i | \vec{x}, \mathbf{W}]$$

where \mathbf{W} is the network weights, \vec{x} is input, L is the length of the correct output, y_i is the i th output character, and \tilde{y}_i is the corresponding correct answer. All models are trained through RMSProp with momentum .95. Every epoch has 10 batches, and every batch has 32 instances of the task. For the LANTM models, after 100 epochs, we half the learning rate if the best error so far is not improved in 30 epochs. The LSTMs are trained with learning rate 0.0002, with no learning rate adjustments during training.

task	model	1x coarse	1x fine	2x coarse	2x fine
copy	LANTM-InvNorm	100%	100%	100%	100%
	LANTM-SoftMax	100%	100%	99%	100%
	LSTM	58%	97%	0%	52%
reverse	LANTM-InvNorm	100%	100%	100%	100%
	LANTM-SoftMax	1%	12%	0%	4%
	LSTM	65%	95%	0%	44%
bigramFlip	LANTM-InvNorm	100%	100%	99%	100%
	LANTM-SoftMax	12%	40%	0%	10%
	LSTM	98%	100%	4%	58%
double	LANTM-InvNorm	100%	100%	100%	100%
	LANTM-SoftMax	100%	100%	100%	100%
	LSTM	98%	100%	2%	60%
addition	LANTM-InvNorm	100%	100%	99%	100%
	LANTM-SoftMax	17%	61%	0%	29%
	LSTM	97%	100%	6%	64%

Table 3: Experiment results. “1 x coarse” and “1 x fine” means the corresponding test scores on input of size same as training input size. “2 x coarse” and “2 x fine” means the corresponding test scores on input twice the size as the training input size. All values are rounded to the nearest integer percent.

Since the training sets are large and separate from the test sets, we train until convergence, testing the models periodically — every 20 epochs for the LANTM models, and every 200 epochs for the LSTM baseline. After training is complete, the best test scores are tabulated.

We tested the models by drawing 100 batches of random problems and computing fine and coarse scores as in [6]. Fine score refers to the percentage of digit or characters (including the EOO marker) that the model correctly outputs. Coarse score refers to the percentage of total problems that the model answers completely correctly.

Tweaks to the LANTM model. We applied two tweaks to the LANTM model described in the previous section: 1) we initialized the mix coefficients for write address and action to strong negative values. This means that the LANTM would tend to write in a straight line. 2) We normalized the step sizes to approximately 1 but did not normalize the initial state step sizes. We found that these two tweaks improved convergence speed and consistency ². Note that with the second tweak, the “group” of actions is no longer a group. This is akin to restricting the head shifts of an NTM to +1 and −1 [5].

5 Results

We trained the models as specified in the last section. The results are listed in table 3.

LANTM-InvNorm was able to master all tasks and generalize nearly perfectly to 2x the training sizes. LANTM-SoftMax did as well on the copy and double tasks but utterly failed at all the others, having performed worse than the LSTM baseline. The baseline itself learned tasks with smaller training input sizes (bigramFlip, double, addition) almost flawlessly, but generalization to 2x training size was pathetic on all tasks, with coarse score not exceeding 6%.

We tested the learned InvNorm model on larger, arbitrarily selected input sizes. The results are summarized by table 4. On permutation tasks, it generalized quite well when challenged by 4 times the training size, able to get more than 90% of test problems correct. On the double task,

²A gif of the read and writes of a LANTM-InvNorm learning the copy task with no biases (tweak 1) is available at <https://gfycat.com/MedicalKeyGalapagostortoise>. Compare with the corresponding gif with biases at <https://gfycat.com/WigglyUnlawfulCaudata>. Details of the gifs can be found in appendix A.

task	4x coarse	4x fine	5x coarse	5x fine	8x coarse	8x fine
copy	100%	100%	91%	100%		
reverse	91%	98%	12%	65%		
bigramFlip	96%	100%			12%	96%
double	86%	99%			21%	90%
addition	2%	95%				

Table 4: Exploring the Generalizability of LANTM-InvNorm. The “ n x coarse” and “ n x fine” refer to the scores with respect to n times the training input size. More specifically, if the LANTM was trained on size 2 to m , then “ n x coarse” means the score it gets when fed inputs of size $(n - 1) \times m + 1$ to $n \times m$. The n s were selected arbitrarily.

its extrapolation performance was similar, with 86% coarse score on 4x training size. Notice that LANTM-InvNorm on several of the tasks (8x bigramFlip, 8x double, 4x addition) achieved high fine scores when extrapolating to large input sizes despite having low coarse scores. This suggests that the extrapolation errors systematically occur at the end of each output on those tasks.

We have created gifs of the read and write locations of LANTM-InvNorm and LANTM-SoftMax while learning each of the 5 tasks, tracking their progress over time. They are available at https://gfycat.com/geyang/lie_access_neural_turing_machine, with details explained in appendix A. One sees clearly that LANTM-InvNorm learned to write in a straight line (which is not surprising given our tweaks to the model) and then read along that same line. On the other hand, LANTM-SoftMax tended to quarantine its read locations to one end of the write line in the reverse, bigramFlip, and addition tasks. In the copy and double tasks, the read line doesn’t stick to the write line as closely with LANTM-Softmax as with LANTM-InvNorm. This is expected since SoftMax assigns a memory vector with high value just if its location a is closer to the read location k than any other memory vector, whereas InvNorm requires k to be very close to a .

In appendix B, we look at the behaviors of trained LANTM-InvNorm through their read and write locations, gate values, and example input/output to analyze what exactly did they learn and where their extrapolation errors come from when challenged by extreme input lengths.

6 Related Works and Comparison of Results

Many recent works have been devoted to the research of external memories and learning algorithmic tasks. We briefly summarize some of the most relevant below, and collected results of experiments similar to our copy and addition tasks in table 5.

LSTM-based models. Zaremba et al. [19] taught LSTM to evaluate simple python programs via curriculum learning, which included copy and addition tasks. They reported 99% accuracy in the addition of 9-digit integers but trouble with copying long sequences. Their version of the tasks had Python programs as inputs, like “print((125+203))” for addition (thus differing from our interleaved inputs in the addition task) and “print(2053)” for copy (thus with much smaller vocabulary — 10 — than in our copy task — 128). They also relied on *teacher forcing*, that is, “even if the LSTM made an incorrect prediction in the i th output digit, the LSTM will be provided as input the correct i th output digit for predicting the $(i + 1)$ th digit” [19]. In contrast, in our experiments, we made no indication of the correct answer during the response phase. Nevertheless, LANTM-InvNorm was able to not only learn 16-digit addition but also correctly answer 32-digit problems 99% of the time, and it had no difficulty with copying long sequences.

In *Grid Long Short-Term Memory* [9], Kalchbrenner et al. arranged LSTM cells in a multidimensional grid which can take as input higher dimensional data such as images. They trained the machine in 15-digit addition (with inputs separated, unlike in this paper) and length 20 copy tasks. Their best model achieved $> 99\%$ accuracy only with 18 layers of 400 cells each and .55 million

	Copy	Vocab	Addition
LSTM [19]	35	10	9
Grid LSTM [9]	20	64	15
NTM [5]	20;20*	256 [†]	-
Neural DeQue [6]	64;128	128	-
LANTM-InvNorm	64;128	128	16;32

Table 5: Comparison of results from other works. For an entry in the “Copy” or “Addition” columns in the form A[B], A indicates the input length such that the model was able to learn to 99% accuracy, either coarse or fine, and B, if present, indicates the input length for which the model can generalize to with accuracy 99%, either coarse or fine, when trained on input length A. The “Vocab” column indicates the vocabulary size used for the copy tasks. We chose 99% as a threshold because 99% fine accuracy differs very little from 99% coarse accuracy, which bridges the different accuracy metrics between studies. We chose only the copy and addition tasks as those are the ones most replicated among different papers. There are nontrivial differences in experimental setup between different papers, which are explained in the text. Thus it must be duly noted that this table is only meant for a rough comparison, which ultimately lacks the rigor provided by a head-to-head experiment containing all of these models. The asterisk (*) indicates that [5] gave no statistics on the actual performance comparable to the fine and coarse scores here, but here we assume that sample input/output of figure 4 of that paper is illustrative of NTM’s performance on the copy task. The dagger ([†]) indicates that NTM’s copy task has input and output symbols encoded in 8-bit strings, thus with an effective vocabulary size of 256, compared to all other studies having input and output symbols represented via one-hot encodings.

samples on the addition task, while, if we assume for the moment that the experimental conditions are close enough to allow meaningful comparison, our LANTM-InvNorm learned 16-digit addition with about .16 million samples and orders of magnitude less parameters, and generalized to 32 digit-addition with 99% accuracy. Similarly, their best model reached 100% accuracy in the copy task with many more parameters and samples than our LANTM-InvNorm used to do the same, despite their machine only having to copy length 20 sequences compared to (up to) 64 in our version.

NTM-based models. As mentioned in the introduction, Graves et al. [5] constructed the Neural Turing Machine by tying an LSTM or feedforward controller to a fixed size memory array via read and write heads. These heads are responsible for taking and carrying out read and write instructions from the controller. An important feature is that the model is differentiable end-to-end, allowing it to be trained via gradient-descent methods. Our LANTM model adopts the core ideas of NTM, but with the following important differences: 1) NTM’s hardwired content addressing system is replaced by LANTM’s key system that gives each memory vector a key, or address, in an Euclidean space \mathbb{R}^n . 2) NTM moves its head location, which is a probability vector over the memory slots, via convolution with another probability vector, but LANTM does so by emitting a Lie action that acts upon its head location, which is a coordinate in \mathbb{R}^n . In the implementation of this paper, this only involves computing a translation 2-vector and adding it to the 2-vector head location, which can be done much more quickly than a convolution of two size-128 vectors. 3) There is no bound on the number of memory vectors LANTM can have. 4) There is no erasure function in LANTM.

Graves et al. tested NTM on a copy task very similar to ours, with no input during the response phase, but all input and output are in bit strings. They used a memory array of 128 memory vectors each of dimension 20 in order to learn length 20 copy task, with good but imperfect generalization to length 30, 50, and 120 ³. LANTM used half the memory size (about 64×20 , as the input is only about length 64, and a new memory vector is created for each input character) to learn length 64 copy task, generalizing to length 128 and 256 perfectly, and even with 91% coarse accuracy and 100% fine accuracy on length 320. One caveat here is that each symbol in NTM’s copy task is an 8-bit

³[5] gave no statistics on the actual performance comparable to the fine and coarse scores here, but here we assume that sample input/output of figure 4 of that paper is illustrative of NTM’s performance on the copy task.

string, so its effective vocabulary size is 256, compared to 128 atomic symbols in our experiment.

In *Learning to Transduce with Unbounded Memory*, Grefenstette et al. [6] designed smooth versions of stack, queue, and deque as external memories to an LSTM controller, and these models were respectively named the Neural Stack, Queue, and DeQue. The models have the distinguishing property of having constant time access to their external memories, which were also unbounded, like LANTM. The models were trained on the copy, reverse, and bigramFlip tasks, and we adopted their setup in this paper for the most part; the other tasks in that paper were two transduction tasks with synthetic grammars. The Neural DeQue was able to learn and generalize all tasks except bigramFlip. In contrast, LANTM-InvNorm excelled at all three permutation tasks with a much smaller model size, with the caveat that our bigramFlip task was half the size of that in Grefenstette et al.

In *Reinforcement Learning Neural Turing Machines*, Zaremba et al. [20] tweaked the NTM model so that it does not need to involve the entire memory array every time memory is accessed. This was done via an intricate application of reinforcement learning, and the model is named RL-NTM. They had RL-NTM learn simple sequence tasks like reverse and repeatCopy with modest success.

Others. Weston et al. [18] wrote about ideas similar to those in *Neural Turing Machines* in the paper *Memory Networks*, released around the same time. They gave a general construction of a machine with external memory and implemented a specific version, testing it on QA tasks. Sukhbaatar et al. [14] improved upon the paper to give a memory network trainable via gradient descent end-to-end, and obtained good results in language modelling along with weaker results in QA. Kumar et al. [11] added a episodic memory module on top of a memory network to be able to recursively focus on parts of specific facts relevant to the question at hand.

7 Discussion

Two things about our experimental results are unusual in view of the current trend in neural network research. One is that the go-to method for assigning weights — the softmax layer — could not yield effective learning of tasks other than the relatively simple copy and double tasks. The other is that our key space, \mathbb{R}^2 , was surprisingly effective, when one perhaps would at first picked a relatively large dimension.

We are uncertain what factors contribute to these phenomena, but nevertheless here mention some possible starting points to look into.

InvNorm performs better. Recall that InvNorm has the following formula

$$w_r^{(t)}(i) := \frac{S^{(t)}(i) \|k_r^{(t)} - a^{(t)}(i)\|^{-2}}{\sum_j S^{(t)}(j) \|k_r^{(t)} - a^{(t)}(j)\|^{-2}}$$

where $a^{(t)}(i)$ is the address of and $S^{(t)}(i)$ is the memory strength of the memory vector $M^{(t)}(i)$. Notice $w_r^{(t)}(i) \rightarrow 1$ for some i only when $k_r^{(t)} \rightarrow a^{(t)}(i)$. Thus reading a memory with high fidelity means that the read location must be very close to the memory location. But when $k_r^{(t)}$ is far from all points $a^{(t)}(i)$, $w_r^{(t)}(i)$ tends to the uniform distribution. Consider a simplified memory retrieval setting where a controller tries to emit an address k such that the resultant memory vector ρ produced by the InvNorm scheme minimizes the squared error $\|\rho - M^{(t)}(i)\|^2$ for some i . If memory vectors are linearly independent, then $k = a^{(t)}(i)$ is the unique global error minimizer, with error 0. This means that, at least for k in a neighborhood of $a^{(t)}(i)$, the gradient of k (under regularity conditions) points more or less toward $a^{(t)}(i)$, and the controller will eventually, under gradient descent, hone k in toward $a^{(t)}(i)$.

On the other hand, SoftMax has the formula

$$w_r^{(t)}(i) := \frac{S^{(t)}(i) \exp(-\|k_r^{(t)} - a^{(t)}(i)\|^2/T^{(t)})}{\sum_j S^{(t)}(j) \exp(-\|k_r^{(t)} - a^{(t)}(j)\|^2/T^{(t)})}$$

so $w_r^{(t)}(i) \rightarrow 1$ for some i only when $\|k_r^{(t)} - a^{(t)}(i)\|$ is much smaller than $\|k_r^{(t)} - a^{(t)}(j)\|$ for all $j \neq i$. Naturally then, there are decision regions $R_i \in \mathbb{R}^n$ such that $k_r^{(t)} \in R_i$ implies $\operatorname{argmax}_j w_r^{(t)}(j) = i$. Reading a memory with high fidelity with SoftMax only requires that the read location be in the interior of some decision region, far enough from the decision boundaries, and the temperature $T^{(t)}$ is sufficiently low. In the memory retrieval setting described above (modified so that the controller now emits also a temperature T for use in the SoftMax scheme), there is no longer a global minimum (k, T) minimizing the squared error; any such “minimum” would take T to infinity, while k just needs to be within the appropriate decision region for $M^{(t)}(i)$. Within the wider setting of LANTM learning via BPTT, this inability to precisely hone in on $a^{(t)}(i)$ can negatively impact the precision of Lie access.

For example, suppose we have memory vectors $M(j)$ stored at $a(j)$ in a straight line at regular intervals, and the task is to output $M(1), M(2), \dots, M(m)$ in order. Under gradient descent, LANTM-InvNorm is likely to learn the addresses of two consecutive memories, from which it learns the Lie action step that connect every pair of consecutive memories (here we are appealing more to intuition than rigor). This allows the machine to quickly learn to traverse the entire memory array. But LANTM-SoftMax cannot follow the same strategy as it has less propensity to learn the exact addresses, and therefore less propensity to learn the Lie action step between consecutive memory addresses. In short, while InvNorm makes it harder to retrieve individual memories by requiring the emitted keys to be exact, this same requirement makes it easier to go from one memory location to the next.

Plausibly, this difference between InvNorm and SoftMax is magnified when the task at hand becomes more complicated, causing the perceived differences in experimental results in tasks like addition.

\mathbb{R}^2 works well. We cannot quite explain why \mathbb{R}^2 as key space has induced good performance, but we can take an educated guess as to the difference between high and low dimensions in regards to InvNorm.

Under InvNorm, a high dimension n (possibly) makes memory retrieval of any particular memory vector $M^{(t)}(i)$ more difficult. Indeed, to read $M^{(t)}(i)$ with high fidelity, the read key must be very close to $a^{(t)}(i)$ for all n of its coordinates, which is certainly easier for small n than for large n .

Whatever the reason, the fact that \mathbb{R}^2 serves as a good key space has allowed good visualization of the memory operations in a LANTM, not only over the course of its execution but also over its evolution through training (see appendix A). This opens up the possibility of monitoring training progress through real time (per epoch) visualization of a LANTM’s reads and writes, which can give a better indication of training set performance than the error suggests. Indeed, the author has implemented such a system, and the gifs in appendix A are essentially the real time visualizations strung together.

Based on our experimental results, LANTM has potential for application to episodic tasks like machine translation of sentences or question answering. However, the fact that the memory is unbounded limits its applicability in continuous tasks like modeling large corpus of text. In the future, we hope to develop a version of bounded memory for such applications. Possible ideas include discounting the memory strength exponentially through time according to disuse and removing all memories with strength less than a threshold, or fixing the memory locations beforehand and use InvNorm to compute memory weights, similar to how NTM uses cosine-distance and SoftMax to perform content addressing.

Nevertheless, it is important to note that in episodic tasks, LANTM’s memory usage may be no larger, or even smaller, than comparable fixed memory systems. For example, the NTM of [5] used a memory array of 128 memory vectors each of dimension 20 in order to learn length 20 copy task, but LANTM used only half the memory size (about 64×20 , as the input is only about length 64, and a new memory vector is created for each input character) to learn length 64 copy task.

While LANTM has succeeded in all of the tasks here, what is perhaps dissatisfying is that its strategy remains more or less the same: writing and reading in a straight line. This begs question,

can LANTM learn tasks for which this strategy is no longer adequate? If not, what modification can be made toward this end? These are topics for further investigation, and we already have some nascent ideas on expanding and tweaking the LANTM model: 1) adding a “content” addressing system, for example, as in NTM; 2) researching an efficient and effective erasure mechanism; 3) trying other Lie groups, such as other subgroups of the Mobius transformation group, and seeing if another smooth manifold works better than \mathbb{R}^n as the key space.

8 Conclusion

Our experiments showed that, in the 5 tasks selected, a small LANTM-InvNorm was able to learn and generalize almost perfectly, while the large LSTM baseline failed in many of them. In addition, InvNorm was clearly better than SoftMax as a weight scheme, as LANTM-SoftMax could not learn or generalize tasks other than copy and double.

Our results suggest that a smooth key space, with no fixed bound on the number of memories, dramatically increases the learnability and generalizability of problems involving long term correlations — but only with the right weight scheme.

References

- [1] Dzmitry Bahdanau, Kyunghyun Cho, and Yoshua Bengio. Neural Machine Translation by Jointly Learning to Align and Translate. *arXiv:1409.0473 [cs, stat]*, September 2014. arXiv: 1409.0473.
- [2] Kyunghyun Cho, Aaron Courville, and Yoshua Bengio. Describing Multimedia Content using Attention-based Encoder–Decoder Networks. *arXiv:1507.01053 [cs]*, July 2015. arXiv: 1507.01053.
- [3] Kyunghyun Cho, Bart van Merriënboer, Caglar Gulcehre, Dzmitry Bahdanau, Fethi Bougares, Holger Schwenk, and Yoshua Bengio. Learning Phrase Representations using RNN Encoder-Decoder for Statistical Machine Translation. *arXiv:1406.1078 [cs, stat]*, June 2014. arXiv: 1406.1078.
- [4] Alex Graves, Abdel-rahman Mohamed, and Geoffrey Hinton. Speech Recognition with Deep Recurrent Neural Networks. *arXiv:1303.5778 [cs]*, March 2013. arXiv: 1303.5778.
- [5] Alex Graves, Greg Wayne, and Ivo Danihelka. Neural Turing Machines. *arXiv:1410.5401 [cs]*, October 2014. arXiv: 1410.5401.
- [6] Edward Grefenstette, Karl Moritz Hermann, Mustafa Suleyman, and Phil Blunsom. Learning to Transduce with Unbounded Memory. *arXiv:1506.02516 [cs]*, June 2015. arXiv: 1506.02516.
- [7] Sepp Hochreiter and Jürgen Schmidhuber. Long Short-Term Memory. *Neural Comput.*, 9(8):1735–1780, November 1997.
- [8] Rafal Jozefowicz, Wojciech Zaremba, and Ilya Sutskever. An Empirical Exploration of Recurrent Network Architectures. In *Proceedings of the 32nd International Conference on Machine Learning (ICML-15)*, pages 2342–2350, 2015.
- [9] Nal Kalchbrenner, Ivo Danihelka, and Alex Graves. Grid Long Short-Term Memory. *arXiv:1507.01526 [cs]*, July 2015. arXiv: 1507.01526.
- [10] Andrej Karpathy and Li Fei-Fei. Deep Visual-Semantic Alignments for Generating Image Descriptions. *arXiv:1412.2306 [cs]*, December 2014. arXiv: 1412.2306.

- [11] Ankit Kumar, Ozan Irsoy, Peter Ondruska, Mohit Iyyer, James Bradbury, Ishaan Gulrajani, and Richard Socher. Ask Me Anything: Dynamic Memory Networks for Natural Language Processing. *arXiv:1506.07285 [cs]*, June 2015. arXiv: 1506.07285.
- [12] John Lee. *Introduction to Smooth Manifolds*. Graduate Texts in Mathematics 218. Springer, 2 edition, 2012.
- [13] Junhua Mao, Wei Xu, Yi Yang, Jiang Wang, Zhiheng Huang, and Alan Yuille. Deep Captioning with Multimodal Recurrent Neural Networks (m-RNN). *arXiv:1412.6632 [cs]*, December 2014. arXiv: 1412.6632.
- [14] Sainbayar Sukhbaatar, Arthur Szlam, Jason Weston, and Rob Fergus. End-To-End Memory Networks. *arXiv:1503.08895 [cs]*, March 2015. arXiv: 1503.08895.
- [15] Ilya Sutskever, Oriol Vinyals, and Quoc V. Le. Sequence to Sequence Learning with Neural Networks. *arXiv:1409.3215 [cs]*, September 2014. arXiv: 1409.3215.
- [16] Oriol Vinyals, Alexander Toshev, Samy Bengio, and Dumitru Erhan. Show and Tell: A Neural Image Caption Generator. *arXiv:1411.4555 [cs]*, November 2014. arXiv: 1411.4555.
- [17] Paul J. Werbos. Backpropagation through time: what it does and how to do it. *Proceedings of the IEEE*, 78(10):1550–1560, 1990.
- [18] Jason Weston, Sumit Chopra, and Antoine Bordes. Memory Networks. *arXiv:1410.3916 [cs, stat]*, October 2014. arXiv: 1410.3916.
- [19] Wojciech Zaremba and Ilya Sutskever. Learning to Execute. *arXiv:1410.4615 [cs]*, October 2014. arXiv: 1410.4615.
- [20] Wojciech Zaremba and Ilya Sutskever. Reinforcement Learning Neural Turing Machines. *arXiv:1505.00521 [cs]*, May 2015. arXiv: 1505.00521.

Appendices

A Gifs

For each task and each of LANTM-InvNorm and LANTM-SoftMax, we created a gif of sample read and writes over the course of learning; the entire album is available at https://gfycat.com/geyang/lie_access_neural_turing_machine. Each gif was created as follows:

1. At the end of each epoch, we randomly selected an input of the maximum training length specific to that task (for example, in the case of addition task, two 16-digit numbers interleaved).
2. We ran the model, with all weights set as trained so far, on this input and record the read and write locations in the key space, along with the strength of each memory vector.
3. When training is complete, we plot the recording of each epoch in a separate frame, and string them together into a gif file. The write locations are marked by red circles, and filled so that a darker fill color means higher memory strength. The read locations are marked by blue disks and connected together by a blue line chronologically (the read line).

Even though we did not explicitly indicate the directionality of the read line, one may infer the directionality of the write sequence by noting that a red circle with white filling marks the beginning of the writes. Then the read sequence will follow this directionality in all tasks other than the reverse task.

B Close analysis

In this section, we discuss the performance of LANTM-InvNorm through various statistics and example input/outputs.

B.1 Permutation tasks

B.1.1 copy

Figure 7a shows the read and write locations of such a LANTM-InvNorm, trained on length 1 to 64 input, running on a typical length 320 input. As one might expect, the reads and writes proceed along straight lines in the key space. The actual read locations keep close to the corresponding write locations. In this execution, the LANTM made no errors (figure 7c).

Figure 7b shows the values of the 4 gates governing the computation of read and write keys. A value of 0 means the gate takes the previous step or key location, while a value of 1 means the gate takes the newly computed step or key location. While the write location gates during the input phase and the read location gates during the response phase were as expected pushed to 0, the write step and read step gates were unexpectedly pushed to 1. Thus the LANTM must have memorized a fixed step size and used it for both reads and writes.

B.1.2 reverse

The counterparts of these graphs for the reverse task are exhibited in figure 8. On the left we have data for length 128 input, demonstrating a correct execution, while on the right we have data for length 300 input, demonstrating what goes on when extrapolating to higher input sizes.

We see that LANTM trained on the reverse task functions much like that trained on the copy task, with read and write heads traversing on straight lines, except now the directionalities are opposed. However, when running on length 300 input, the read line, i.e. the curve connecting the read locations in sequence, bends suddenly toward the end, causing almost all reads at the end to diverge from the writes and making almost all outputs at the end to be incorrect. This is somewhat surprising, for one might have expected error to come in the form of the accumulation of a small difference between the slopes of the read and write lines. Along with the sudden dip in read step gate value at the end (blue line in figure 8d), the bending of the read line suggests that the LSTM controller started to forget its learned program as the answering phase drew toward a conclusion.

B.1.3 bigramFlip

The same phenomena appear with the bigramFlip task, where reads and writes happen along 2 closely aligned lines, but when tested by a long input, the reads will abruptly fall out of order: while in the reverse task, the read line visibly bends away from the write line, here the lines stay straight but each step in the read line is elongated, starting around the 187th read (figure 9b).

One might be surprised to see that the read happens along a line instead of zigzagging inside the write line. On closer inspection, we find that LANTM works as follows:

1. LANTM stores representations of the inputs in input order.
2. Meanwhile it memorizes the first two input characters and outputs them in the reverse order after reading the first two EOI symbols.
3. When it sees the first EOI symbols, it starts reading the second bigram, i.e. it reads characters 3 and 4 (or their representations in memory; this corresponds to the 5th and 6th memory vectors) after seeing the first and second EOI symbols. This effectively allows it to “look ahead” and have each bigram on hand before having to output the flipped image of it.

4. The LSTM flips each “look ahead” bigram and outputs it in order. Repeat for each bigram.

Unique to the LANTM trained on bigramFlip is the oscillation of the read step gate between 0 and 1 (figure 9c and 9d). This seems like more an artifact of the learning process than a feature of the learned computation, as it would also imply that the controller memorized a single fixed read step, and that the error that occurs with extrapolation seems to stem from the adulteration of this memory.

B.2 Arithmetic tasks

In the double task, the LANTM behaved much like it did in the copy task. It stored the input in a line and then computed the doubling with carry digitwise.

In the addition task, the LANTM learned to compress each pair of digits of the input numbers (which, as mentioned above, are interleaved) and store them in the odd write locations; the even write locations had vanishing memory strength (figure 11a and 11b). The LANTM then read off the information by skipping through the odd memory locations.

As with copy and reverse tasks, the read step gate values during the response phase were all close to 1, meaning that the LANTM kept the read step in the LSTM controller memory. This suggests that the read step gate might be an unnecessary design.

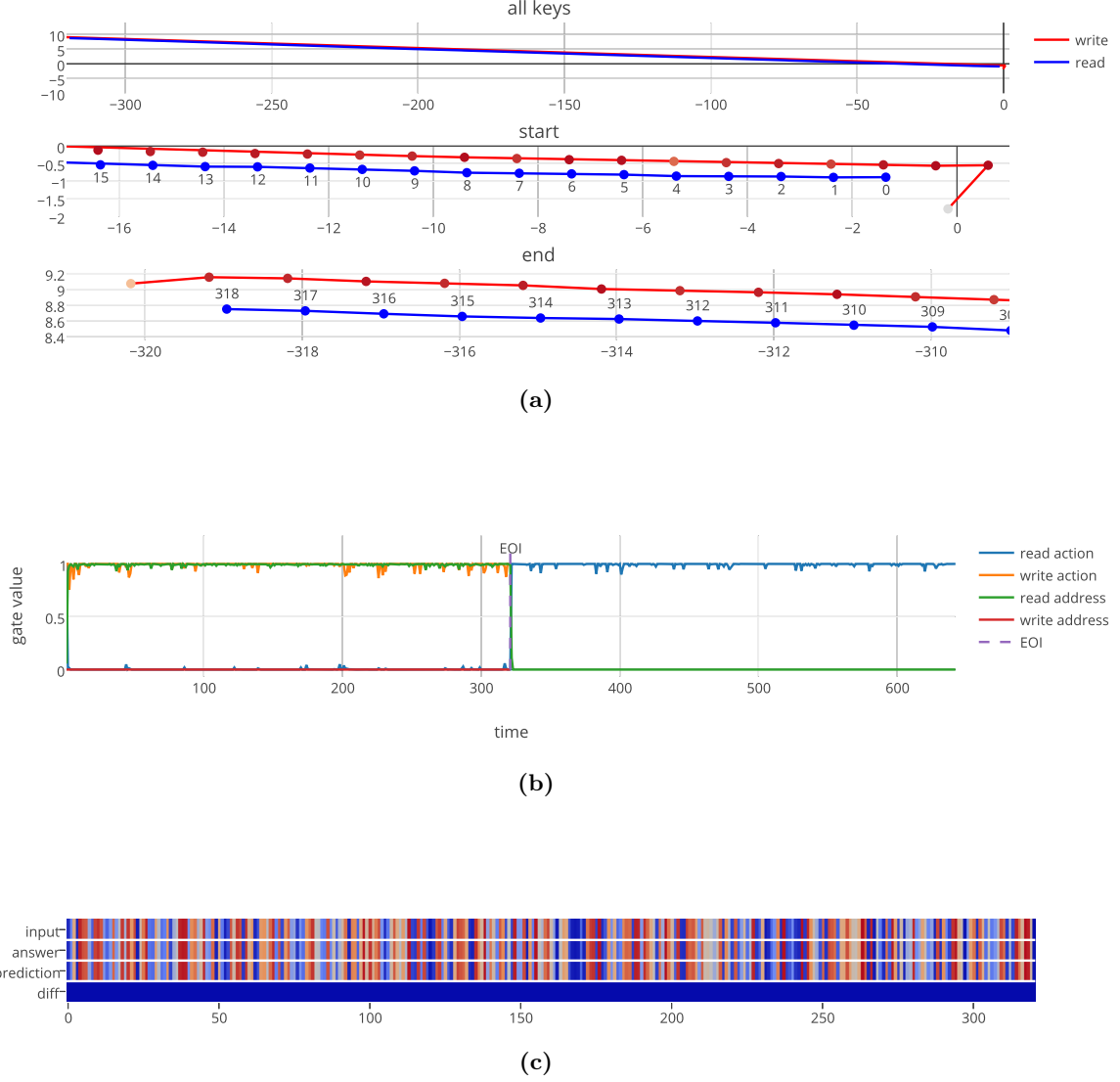


Figure 7: Copy task with length 320 input. Here, a LANTM-InvNorm trained on the copy task of length 1-64 inputs is executed on a length 320 input. **(a) read and write locations.** These are 3 views of the read and write locations of the LANTM. Red represents write locations, and blue represents read locations. Only the read locations during the response phase and which are used to compute nonmarker outputs are shown here. For each red dot, the darker the color the higher the corresponding memory strength. The scale ratios are all approximately 1:1, i.e. a 1x1 square according to the ticks on the x and y axes should appear as a square. The subplots, top to bottom, respectively show an overview, the beginning, and the end of the read and write locations in chronological order. Numbers 0 to 319 label the read keys in this order. More precisely, read key i is emitted when the LANTM reads the i th EOI symbol (so that the actual value read is fed back into the LANTM at time $i + 1$). **(b) gate values during the execution** The vertical dashed line in the middle (slightly hard to see due to overlap with the green trace) marks the time when the LANTM reads the EOI symbol. **(c) correct answer, LANTM's prediction, and the difference.** Each different color represents one of the 128 possible values of the vocabulary. The first row is the correct answer, the second row LANTM's prediction, and the third the difference between the two. In the third row, at most two colors are present: blue means LANTM's response is correct; red means incorrect. In this case there are no red bars because the LANTM was able to perfectly copy the input.

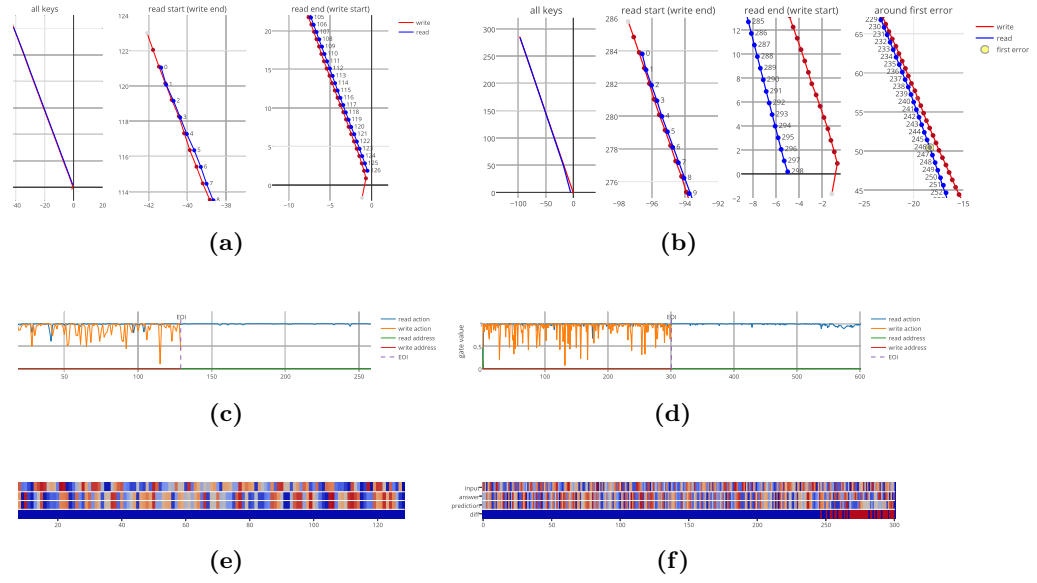


Figure 8: Reverse task with length 128 and 300 inputs. The left side shows data on length 128 input; the right side, length 300. Graph formats are the same as in figure 7, except that in subfigure 8b, there is now a fourth plot showing keys around where LANTM made the first mistake. This spot is marked by a yellow dot.

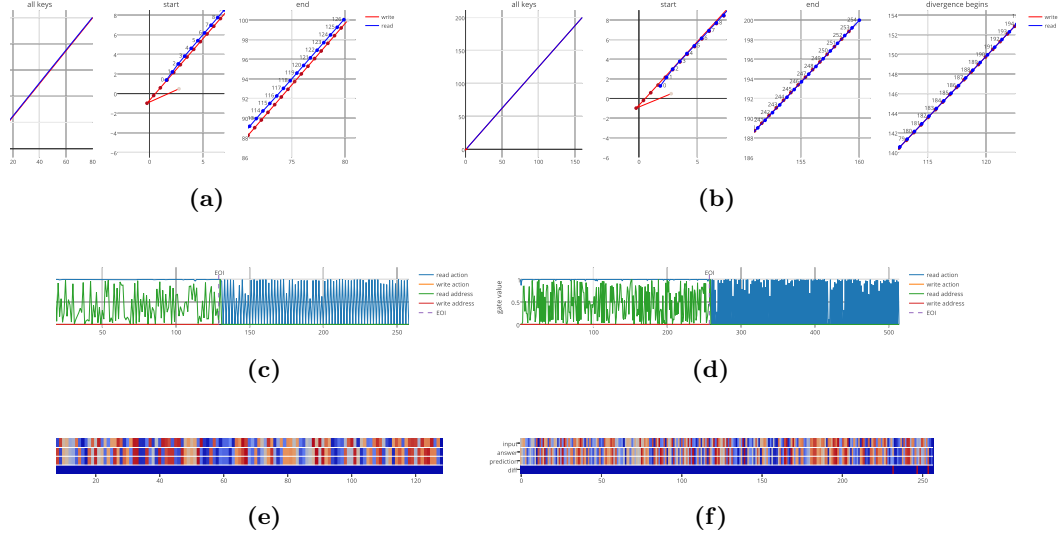


Figure 9: Bigram flip task with length 128 and 256 inputs. The left side shows data on length 128 input; the right side, length 256. Graph formats are the same as in figure 7, except that in subfigure 9b, there is now a fourth plot showing keys around where the reads start to diverge from the writes. In the gate value plots, the write step lines (orange) are almost constant at 0, hidden behind the red lines (write location).

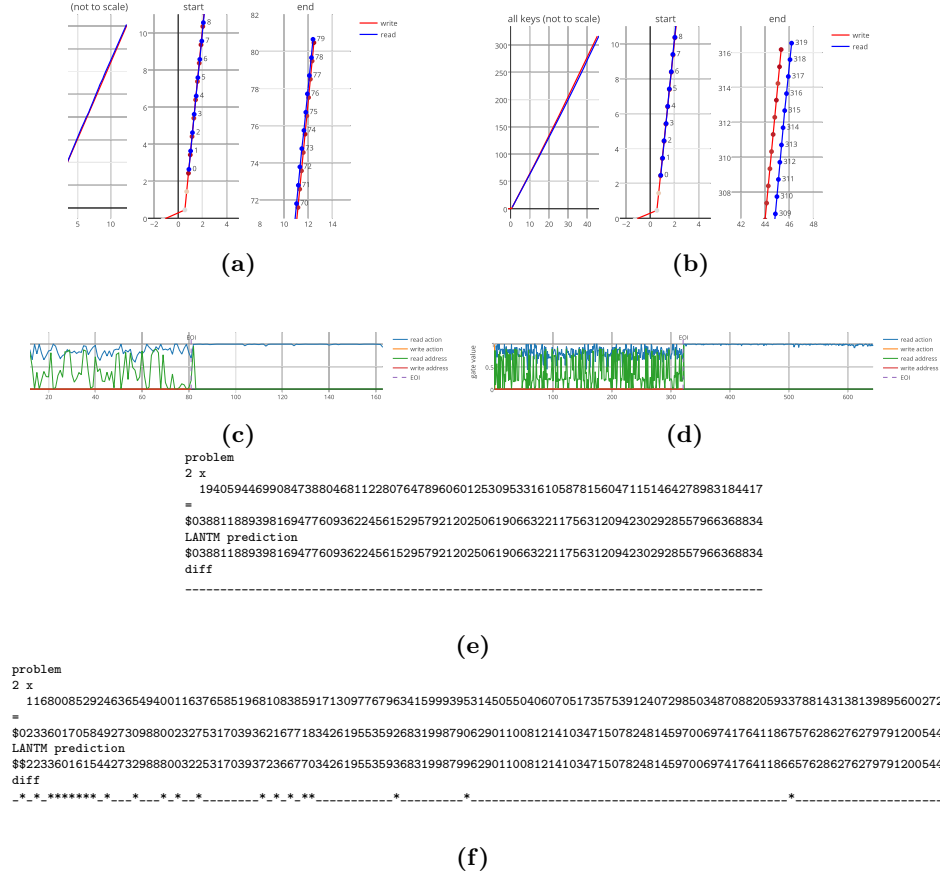


Figure 10: Double task with length 80 and 320 inputs. The subfigures a, c, e show data on length 80 input; the subfigures b, d, f, length 320. Graph formats for the first two rows are the same as in figure 7, except that in the first row, the overview plots are magnified horizontally to accentuate the divergence of the read and write lines, demonstrating that the divergence is a gradual build up of difference in slope. In the gate value plots, the write step lines (orange) are almost constant at 0, hidden behind the red lines (write location). **10e and 10f.** We show the doubling problems given to the LANTM and its response. Dollar signs (\$) represent the end symbol. Asterisks (*) mark points where LANTM’s answers are incorrect. In e, only the first (most significant) 130 digits are shown, as there are no errors in the remaining digits.

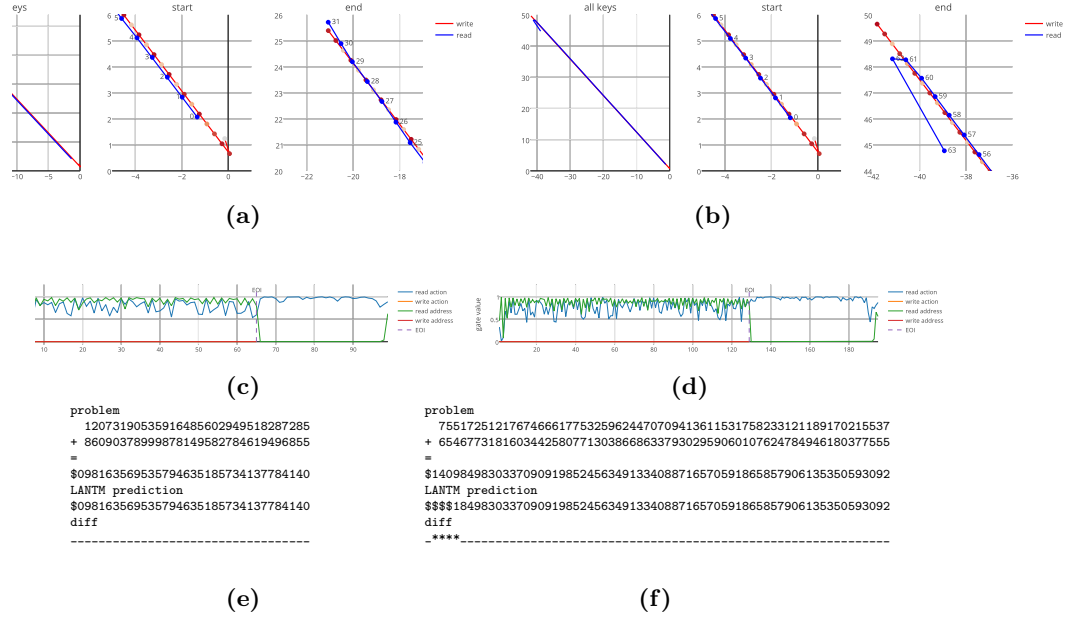


Figure 11: Addition task with 32-digit and 64-digit inputs. The subfigures a, c, e show data on 32-digit input; the subfigures b, d, f, 64-digit. Graph formats for the first two rows are the same as in figure 7. In the gate value plots, the write step lines (orange) are almost constant at 0, hidden behind the red lines (write location). **11e and 11f.** We show the addition problems given to the LANTM and its responses. Dollar signs (\$) represent the end symbol. Asterisks (*) mark points where LANTM’s answers are incorrect.